

AUTOMATIC EDGE DETECTION SOLUTION USING ANISOTROPIC DIFFUSION-BASED MULTI-SCALE IMAGE ANALYSIS AND FINE-TO-COARSE TRACKING

Tudor BARBU

Institute of Computer Science, Romanian Academy – Iași Branch

Corresponding author: Tudor BARBU, E-mail: tudor.barbu@iit.academiaromana-is.ro

Abstract. An automatic multi-scale image edge detection technique is proposed in this research work. The multiscale image analysis used by the proposed approach is based on a nonlinear anisotropic diffusion-based scale-space that is constructed by applying the finite difference method-based numerical approximation scheme of a novel well-posed second-order anisotropic diffusion model. The image boundaries are detected at each scale of the obtained PDE-based scale-space by searching for zero-crossings and applying some gradient magnitude thresholding procedures and morphological operations. The edges determined at multiple scales are then combined, by using a fine-to-coarse edge tracking approach, into the final edge detection result. Some boundary detection simulations and method comparisons that prove the effectiveness of the proposed technique are also provided here.

Key words: edge detection, multi-scale image analysis, nonlinear anisotropic diffusion-based filter, numerical approximation algorithm, fine-to-coarse boundary tracking.

1. INTRODUCTION

Edge detection represents a very important and challenging image analysis domain that has been widely researched in the past 60 years. It includes various techniques that identify the image boundaries, which contain the points in a digital image where its brightness has sharp discontinuities. These edges correspond to the discontinuities in depth or in surface orientation, variations in scene illumination or changes in material properties [1]. This boundary detection area has many image analysis and computer vision applications, since edge information is required in various fields, such as the object detection and tracking, pattern recognition, face, fingerprint and iris detection, biometric authentication, image compression and remote sensing.

A variety of edge detectors have been developed in the last decades. The traditional detectors could be grouped into two main categories. The first one includes the boundary detection techniques based on first-order derivative of the image [2], such as the classical gradient operators introduced by Roberts, Sobel and Prewitt. The second category includes the detection approaches based on the second-order derivative [3], such as the Laplacian of a Gaussian (LoG) – based edge operator proposed by Marr and Hildreth [4]. The most popular edge detector, which still represents the state-of-the-art in this field, is the multi-stage image boundary detection algorithm developed by J. Canny [5].

Since the image edges represent multi-scales structures in nature and the human vision has also a multi-scale character, a variety of multi-scale edge detection solutions have been proposed in the last years [6]. The multi-scale and multi-resolution image analysis has been applied successfully to many image processing and computer vision tasks, providing better results than the traditional approaches in these domains. The multi-scale representations represent better solutions to extract the boundaries in natural scenes and work properly in noisy conditions, reducing considerably the white additive image noise. The early work on multi-scale edge detection used 2D Gaussian filtering at multiple scales given by σ , and fine-to-coarse and coarse-to-fine boundary tracking procedures [7, 8]. The edge focusing techniques represent more performant methods that detect the edges in a image filtered by a large scale Gaussian filter, by using adaptive thresholding, and then combine the edge information by moving from a coarse-to-fine scale [9]. Another improved multiscale

edge detection technique, proposed by Williams and Shah [10], used the motion information of the boundaries filtered by a Gaussian operator of different sizes, in order to determine how to link the edge points detected at various scales. A multi-scale extension of the single-scale Sobel detection technique, which is based on Gaussian 2D smoothing and fine-to-coarse edge tracking, was proposed in [11]. The multi-scale anisotropic Gaussian kernels (AGKs) represent another effective solution for image boundary detection [12]. Besides the Gaussian-based approaches, multi-scale edge detection techniques using other filtering solutions have been developed. Thus, some effective multi-scale boundary extraction methods are based on Wavelet transforms [13, 14]. Other multiscale edge detection algorithms use nonlinear partial differential equation (PDE)-based filters, such as the influential anisotropic diffusion scheme introduced by Perona and Malik [15]. The PDE variational models have been also used by the image edge detection techniques based on active contour models [16, 17].

We also consider a nonlinear PDE-based edge-based image segmentation approach in this paper. So, we proposed some anisotropic diffusion-based [18] and active contour (level-set) based [19] boundary detection techniques in our past works. Here we introduce a novel multi-scale edge detection framework based on a well-posed second-order nonlinear anisotropic diffusion-based model that is detailed and then solved numerically in the next section. The scale-space representation constructed using the finite difference-based approximation algorithm that solves this PDE model, and the fine-to-coarse edge tracking algorithm combining edges identified at multiple scales are described in the third section. Our numerical experiments and method comparison are discussed in the fourth section and the conclusions are drawn in the final section.

2. NONLINEAR ANISOTROPIC DIFFUSION SCHEME FOR MULTISCALE IMAGE ANALYSIS

The proposed edge detection framework uses a multiscale image analysis based on anisotropic diffusion. A nonlinear diffusion-based filtering approach is used to create the scale-space representation, since it provides more efficient scale spaces than the classic 2D Gaussian filter. The considered PDE-based filter is described in the next subsection and its numerical approximation is performed in the subsection 2.2.

2.1. Parabolic second-order PDE-based denoising model

We have conducted a high amount of research in the PDE-based image restoration domain, many anisotropic diffusion and variational denoising models being developed by us in the last decade [20]. Some of them have been used for multi-scale analysis [21]. Here we introduce a nonlinear second-order anisotropic diffusion-based filtering model that is composed of the following parabolic partial differential equation and its boundary conditions:

$$\begin{cases} \frac{\partial u}{\partial t} - \beta \delta(\|\nabla u\|) \operatorname{div}(\varphi(\|\nabla u_\sigma\|) \nabla u) + \alpha(u - u_0) = 0, & \forall (x, y) \in \Omega \\ u(0, x, y) = u_0(x, y), & \forall (x, y) \in \Omega \\ u(t, x, y) = 0, & \forall (x, y) \in \partial\Omega; \end{cases} \quad (1)$$

where the parameters $\alpha \in (0, 0.3)$, $\beta \in [1, 2)$, $\Omega \subseteq \mathbb{R}^2$ represents the image domain, the observed image is $u_0 \in L^2(\Omega)$ and $u_\sigma = u * G_\sigma$, where $G_\sigma(x, y) = \frac{1}{2\pi\sigma^2} e^{-\frac{x^2+y^2}{2\sigma^2}}$ is a 2D Gaussian filter kernel. We propose the next diffusivity function, which is positive, monotonic decreasing and converges to 0, for the PDE model (1):

$$\varphi: [0, \infty) \rightarrow [0, \infty): \quad \varphi(s) = \xi \sqrt[3]{\frac{\lambda}{|\eta s^2 + \gamma|}}, \quad (2)$$

where $\eta \in (0, 1]$, $\gamma \geq 4$, $\xi \geq 1$ and $\lambda \geq 5$. The component $\delta(\|\nabla u\|)$ has the role of controlling the speed of this diffusion procedure. The positive function used by it has the following form:

$$\delta: [0, \infty) \rightarrow [0, \infty): \delta(s) = \left(\frac{\varepsilon s^\tau + \zeta}{\nu} \right)^{\frac{1}{\tau+1}}, \quad (3)$$

where $\varepsilon, \zeta \in [1, 5)$, $\nu \in (0, 0.5)$ and $\tau \in (0, 1)$.

So, the nonlinear PDE model given by (1)–(3) combines the anisotropic diffusion to a 2D Gaussian filter in order to achieve an effective white additive noise removal. The diffusivity function given by (2) is properly chosen for an efficient denoising [15, 20]. This PDE-based filter removes successfully the white additive Gaussian noise (AWGN) from the image and preserves and sharpens its boundaries that have to be detected. It overcomes the undesired side effects, such as the image blurring.

This second-order nonlinear diffusion-based model is non-variational, since it cannot be derived from the minimization of an energy cost functional. Also, the proposed PDE model is well-posed, since it exists a unique weak, or variational, solution, for it. That solution is computed numerically by applying a numerical approximation algorithm for (1) that converges to it. This discretization scheme that solves numerically the PDE model is detailed in the next subsection.

2.2. Numerical approximation algorithm

The considered nonlinear anisotropic diffusion-based model is then solved numerically using an approximation scheme that is constructed by applying the finite difference method [22]. Thus, one quantizes the spatial coordinates as $x = ih$, $y = jh$, $i \in \{1, \dots, I\}$, $j \in \{1, \dots, J\}$ and the time coordinates as $t = n\Delta t$, $n \in \{0, \dots, N\}$, where h is the space size and Δt is the time step of the considered grid and $[Ih \times Jh]$ is the dimension of the support image.

Thus, the nonlinear second-order anisotropic diffusion equation given by (1) could be re-written as following:

$$\frac{\partial u}{\partial t} + \alpha(u - u_0) = \beta \delta(\|\nabla u\|) \left(\frac{\partial}{\partial x} (\varphi(|\nabla u_\sigma|) u_x) + \frac{\partial}{\partial y} (\varphi(|\nabla u_\sigma|) u_y) \right). \quad (4)$$

First, one approximates the left component in (4), by using the central finite differences [22], as following:

$$\frac{u_{i,j}^{n+\Delta t} - u_{i,j}^n}{\Delta t} + \alpha(u_{i,j}^n - u_{i,j}^0) = u_{i,j}^{n+\Delta t} \frac{1}{\Delta t} + u_{i,j}^n \left(\alpha - \frac{1}{\Delta t} \right) - u_{i,j}^0 \alpha. \quad (5)$$

Next, the right term of (4) is discretized. The component $\beta \delta(\|\nabla u\|)$ is approximated as $\beta \delta_{i,j} = \beta \delta(\|\nabla u_{i,j}\|)$, and one also computes $\varphi_{i,j} = \varphi(\|\nabla((G_\sigma * u)_{i,j})\|)$, where

$$\|\nabla u_{i,j}\| = \sqrt{\left(\frac{u_{i+h,j} - u_{i-h,j}}{2h} \right)^2 + \left(\frac{u_{i,j+h} - u_{i,j-h}}{2h} \right)^2}. \quad (6)$$

Next, $\frac{\partial}{\partial x} (\varphi(|\nabla u_\sigma|) u_x)$ is discretized spatially as

$\varphi_{i+\frac{h}{2},j} \left((G_\sigma * u)_{i+h,j} - (G_\sigma * u)_{i,j} \right) - \varphi_{i-\frac{h}{2},j} \left((G_\sigma * u)_{i,j} - (G_\sigma * u)_{i-h,j} \right)$ and $\frac{\partial}{\partial y} (\varphi(|\nabla u_\sigma|) u_y)$ is discretized spatially as $\varphi_{i,j+\frac{h}{2}} \left((G_\sigma * u)_{i,j+h} - (G_\sigma * u)_{i,j} \right) - \varphi_{i,j-\frac{h}{2}} \left((G_\sigma * u)_{i,j} - (G_\sigma * u)_{i,j-h} \right)$, where

$$\varphi_{i\pm\frac{h}{2},j} = \frac{\varphi_{i\pm h,j} + \varphi_{i,j}}{2}, \quad \varphi_{i,j\pm\frac{h}{2}} = \frac{\varphi_{i,j\pm h} + \varphi_{i,j}}{2}. \quad (7)$$

One may consider here the values $h = \Delta t = 1$. Then, by using all these discretizations, one obtains the following explicit iterative numerical approximation algorithm:

$$u_{i,j}^{n+1} = u_{i,j}^n (1-\alpha) + u_{i,j}^0 \alpha + \beta \delta_{i,j} \left(\begin{array}{l} \varphi_{i+\frac{1}{2},j} \left((G_\sigma * u)_{i+1,j}^n - (G_\sigma * u)_{i,j}^n \right) - \varphi_{i-\frac{1}{2},j} \left((G_\sigma * u)_{i,j}^n - (G_\sigma * u)_{i-1,j}^n \right) + \\ \varphi_{i,j+\frac{1}{2}} \left((G_\sigma * u)_{i,j+1}^n - (G_\sigma * u)_{i,j}^n \right) - \varphi_{i,j-\frac{1}{2}} \left((G_\sigma * u)_{i,j}^n - (G_\sigma * u)_{i,j-1}^n \right) \end{array} \right) \quad (8)$$

The iterative numerical approximation scheme given by (8) is stable and consistent to the second-order nonlinear diffusion-based model (1) and converges in N steps to its variational solution that represents the smoothing result. This numerical algorithm that solves the PDE-based filtering model is successfully used to construct an effective image scale-space for edge detection that is described in the next section.

3. SCALE-SPACE REPRESENTATION FOR BOUNDARY EXTRACTION

The described nonlinear anisotropic diffusion-based filtering model is used to construct a proper scale-space representation for edge detection. As we already mentioned, the anisotropic diffusion smoothing schemes represent better scale-space creation tools than the 2D Gaussian filter [6, 8].

While the Gaussian operator generates the blurring effect that deteriorates the image boundaries, the anisotropic diffusion-based filters, such as the one proposed here, preserve successfully the edges and other essential details and even enhance them [20]. Also, while the additive denoising using Gaussian filters of increasing variances causes the boundaries to move from their actual locations in the images, the anisotropic diffusion preserves properly the edge localization as the scale is increased.

The proposed anisotropic diffusion-based scale-space is created by applying the nonlinear PDE-based filter (1) on the gray-level image until various moments of time and computing the absolute differences between the filtered images and the initial observation. The iterative numerical approximation algorithm given by (8) is used for this multi-scale image analysis process. Thus, one generates a multi-scale representation with K scales, by considering the smoothing output provided by the numerical scheme (8) at K properly selected iteration moments. The scale-space is obtained as the next set of image subtraction results:

$$S = \left\{ \left| u^\tau - u^0 \right|, \left| u^{2\tau} - u^0 \right|, \dots, \left| u^{K\tau} - u^0 \right| \right\}, \quad (9)$$

where $K \geq 10$, the time step $\tau \in [30, 50]$, u^0 represents the discrete observation and each $u^{k\tau}$, where $k \in \{1, \dots, K\}$, is determined from (8).

An edge detection process based on this scale-space is then performed. So, the image at each k^{th} scale of S , which is denoted $U^k = \left| u^{k\tau} - u^0 \right|$, is then analyzed in order to extract the boundaries at that scale. Thus, the zero-crossing points of U^k are determined first, the binary image representing them being denoted $E(U^k)$. Since we are interested only by those zero-crossings that are essential for the edge detection task, that binary image is further processed. Only the zero-crossing points corresponding to the pixels in U^k that are characterized by a gradient magnitude exceeding a properly selected threshold value are kept in $E(U^k)$. This procedure can be expressed as follows:

$$\left\| \nabla U_{ij}^k \right\| \leq T_k \Rightarrow E(U^k)[i,j] = 0, \quad \forall k \in \{1, \dots, K\}, i \in \{1, \dots, I\}, j \in \{1, \dots, J\}, \quad (10)$$

where $\left\| \nabla U_{ij}^k \right\|$ is computed by (6) and a good threshold value is $T_k = 2\mu \left(\left\| \nabla U^k \right\| \right)$.

Also, because only the real boundaries have to be extracted, our approach discards the very small white spots in the binary image that could represent noise in the grayscale image. Therefore, the connected

components of $E(U^k)$ whose areas (number of pixels) are smaller than a properly chosen threshold c must be removed from it. We have detected empirically an optimal threshold value: $c = 25$.

Next, one applies some morphological operations on the obtained binary image to enhance the edge detection process [23]. Thus, an image closing operation, representing a dilation followed by an erosion, is applied first, as following:

$$E(U^k) := (E(U^k) \oplus Sq) \ominus Sq, \quad (11)$$

where Sq is a $[1 \times 1]$ square structuring element. Next, a morphological thinning process is performed on the closed image given by (11) by applying the Zhang-Suen algorithm [24], its skeleton thus being determined. The obtained thinned $E(U^k)$ image represents the boundary detection result at the k^{th} scale of S . Then, the edges extracted at multiple scales have to be combined into the final boundary detection output. Here we consider a fine-to-coarse edge tracking method for this task. At lower scales, given by small k values, the edge maps $E(U^k)$ correspond to finer image details and some of their white pixels may not represent real edges, but some noise or clutter. At higher scales, given by larger k values, the $E(U^k)$ maps do not contain undesired false edges, but, since they correspond to coarser details, they could miss some real boundaries and dislocate others. So, the proposed edge tracking algorithm starts at the finest scale of S and runs until it reaches the coarsest scale, analyzing all edges of the images of this scale-space and identifying the real ones.

Thus, the boundaries that disappear fast when the scale is increased should be discarded, since they may represent false edges, while those that exist at both fine and coarse scales have to be favored, because they represent salient image structures. So, our fine-to-coarse tracking algorithm considers all the edge (white) pixels of $E(U^1)$ and track them through the scale-space. If they appear in a large enough number of following consecutive edge images $E(U^k)$, they are considered to belong to real boundaries and labeled as such, otherwise they are suppressed. Then, the tracking process continues the same way, by considering the unlabeled edge pixels of $E(U^2)$, tracking them and labeling or discarding them, and so on, until there are not enough remaining scales such that the unlabeled edges of the current $E(U^k)$ to appear in a large enough number of them. A good choice for that number is the ceiling of the half of the total number of scales, $\left\lceil \frac{K}{2} \right\rceil$.

The labeling process means updating a binary matrix that is initialized $E(S) := 0$, by marking with 1 the real edge pixels. This boundary tracking process can be formulated as following:

$$\forall k \in \left\{ 1, \dots, \left\lceil \frac{K}{2} \right\rceil \right\}, i \in \{1, \dots, I\}, j \in \{1, \dots, J\} : E(U^k)[i, j] = \dots = E(U^{k+m})[i, j] = 1 \& m \geq \left\lceil \frac{K}{2} \right\rceil \Rightarrow E(S)[i, j] := 1 \quad (12)$$

Although the proposed anisotropic diffusion-based scale-space representation S preserves the image boundary localization very well, the fine-to-coarse edge tracking process given by (12) could be improved by searching in small edge neighborhoods at higher scales. Thus, to address any possible edge displacement that may occur at large scales, an edge pixel of a map could be accepted as valid even if it is not found at the same location in the edge map of the next scale, but in a 4 or 8-neighborhood of it. That can be formulated as

$$\exists a \in \{i-1, i, i+1\}, b \in \{j-1, j, j+1\} : E(U^k)[i, j] = E(U^{k+1})[a, b] = 1, \forall k \geq \text{high threshold} \quad (13)$$

and may be incorporated in (12). The obtained binary image $E(S)$ represent the final multi-scale edge detection result. It contains the extracted boundaries of the initial observed gray-level image, u^0 .

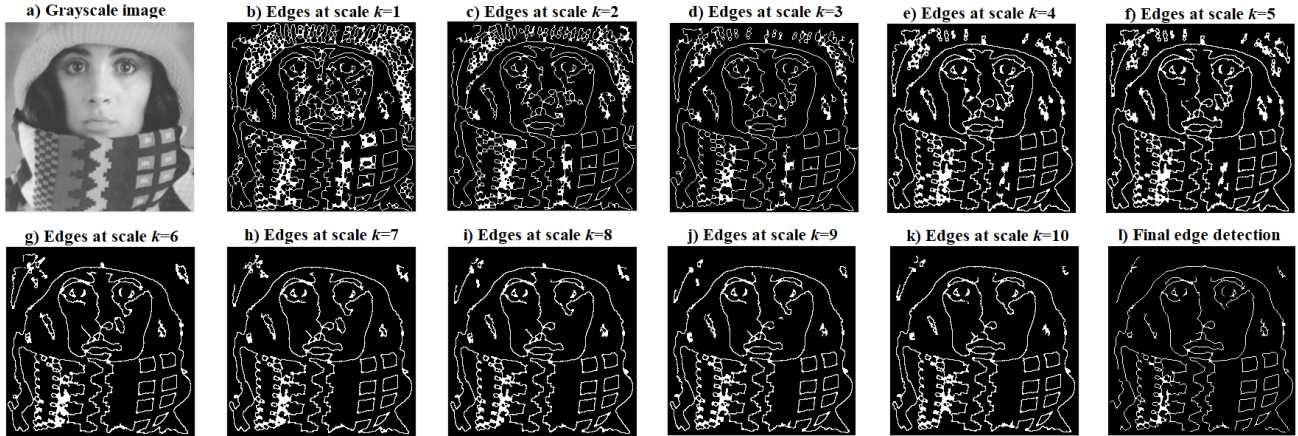


Fig. 1 – Edge detection using a scale-space with $K=10$ scales.

```

Pseudocode EdgeDetection ( $u^0 = [IXJ]$  observed image)
Set  $\tau =$  time step,  $K =$  number of scales;
for  $k=1$  to  $K$ 
 $U^k := |u^{k\tau} - u^0|$ , where  $u^{k\tau}$  is computed by (8);
Compute binary image  $E(U^k) :=$  zero-crossings of  $U^k$ ;
Select proper threshold  $T_k$ ;
for  $i=1$  to  $I$ 
for  $j=1$  to  $J$ 
if  $\|\nabla U_{ij}^k\| \leq T_k$  then  $E(U^k)[i, j] := 0$ ; (see 10)
end
end
Remove very small connected components from  $E(U^k)$ ;
 $E(U^k) :=$  thinning [ $(E(U^k) \oplus Sq) \ominus Sq$ ]; (apply morphological operations)
end
 $E(S) := 0$ , where  $S$  is given by (9);
for  $k=1$  to  $\lfloor \frac{K}{2} \rfloor$ 
for  $i=1$  to  $I$ 
for  $j=1$  to  $J$ 
if  $E(U^k)[i, j] = \dots = E(U^{k+m})[i, j] = 1$  &  $m \geq \lfloor \frac{K}{2} \rfloor$  then  $E(S)[i, j] := 1$ ; (edge tracking process);
end
end
end
Return  $E(S)$ .

```

Fig. 2 – The pseudocode algorithm of the multi-scale image boundary detector.

A multi-scale edge detection example is provided in Fig. 1. The $[256 \times 256]$ *Trui* image displayed in a) is analyzed using the proposed detector. The boundaries extracted at the $K=10$ scales of S are displayed in b)–k) and the final edge detection result is depicted in l). The pseudocode describing all the main steps of this automatic edge detection algorithm is represented in Fig. 2.

4. EXPERIMENTS AND METHOD COMPARISON

The proposed automatic anisotropic diffusion-based multi-scale edge detection approach has been successfully tested on several hundreds of digital color and gray-level images. Some well-known image collections, such as the USC-SIPI Image Database and the Berkeley Segmentation Dataset (BSD), have been

used in our experiments. The boundary detection simulations have been performed using MATLAB on an Intel (R) Core (TM) i7-6700HQ CPU 2.60 GHz processor on 64 bits, running Windows 10.

Given the nonlinear second-order PDE-based filter used to create its scale-space, this multi-scale edge detector identifies properly the image boundaries in both normal and noisy conditions. Because of its high computational complexity, it does not execute very fast. A proper edge detection process requires a number of scales K that cannot be low and a step τ that is quite high. Optimal boundary extraction results have been achieved for $K=15$ and $\tau=40$, which means hundreds of iterations of the numerical approximation algorithm (8). However, the running time of the proposed technique depends on the analyzed image size, too.

The proposed approach has been assessed by applying various evaluation measures that combine the true edge, false edge and missed edge numbers and use the ground truth of the test images, like Precision, Recall, F1, Map Quality (MQ) and Performance Ratio (PR) [25, 26]. The images of the BSD database and the respective ground truths have been used for this method evaluation [26]. Our detection technique achieves satisfactory values of these performance evaluation metrics and Peak Signal to Noise Ratio (PSNR) measure.

Table 1

Method comparison: average PR and PSNR values achieved by several edge detectors

Edge detection technique	Average PR	Average PSNR (in dB)
The proposed multi-scale edge detector	11.0217	20.1742
Canny filter	12.1304	22.3817
Laplacian of Gaussian (LoG)	9.3267	19.4837
Roberts operator	6.5486	15.6745
Sobel detector	7.4251	16.7802
Prewitt filter	8.5139	16.9837

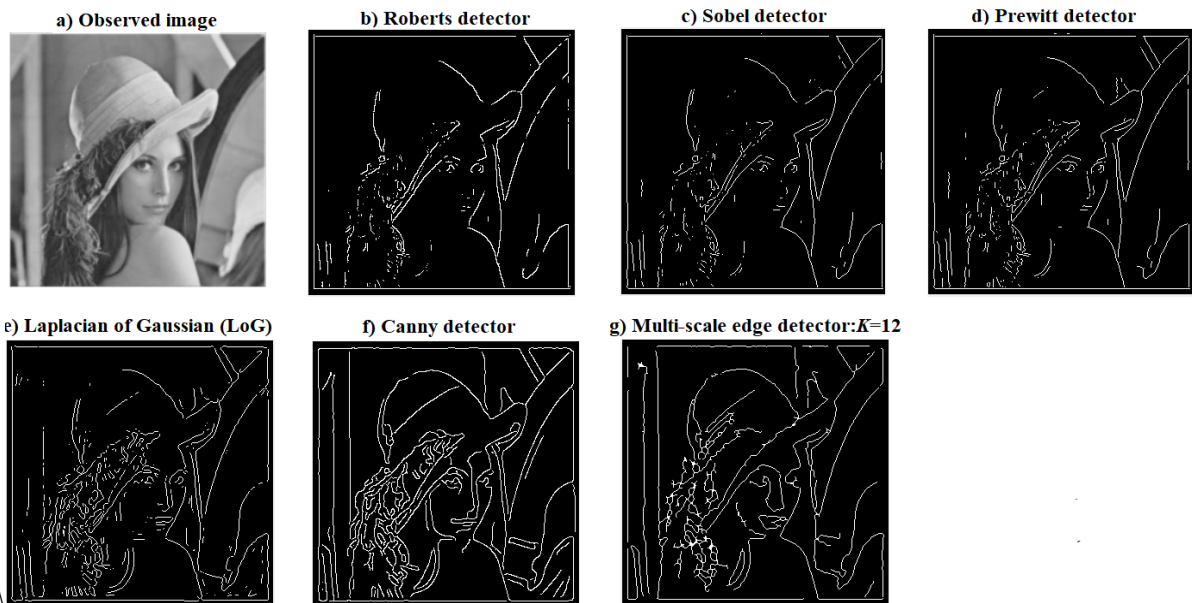


Fig. 3 – Edge detection method comparison example.

Method comparison have been also performed. The multiscale boundary extraction technique proposed here outperforms the classic edge detectors, achieving better values of the performance metrics. Thus, the average PR (the ratio of true to false edges) and PSNR scores obtained for 175 BSD testing images (www2.eecs.berkeley.edu/Research/Projects/CS/vision/bsds) by this anisotropic diffusion-based approach and other edge detection methods are displayed in Table 1. So, the proposed PDE-based multi-scale boundary detector performs better than mono-scale detectors Roberts, Sobel and Prewitt, and even than the Laplacian of a Gaussian (LoG) edge detection filter, achieving higher average PR and PSNR values. It also outperforms a past diffusion-based detector introduced by us [18], but it is slightly outperformed by the still

state-of-the-art Canny filter that obtains somewhat better values of these measures. However, the described algorithm has the disadvantage of running a bit slower than those edge detectors, due to its high complexity.

An edge detection method comparison example is described in Fig. 3. The edges of grayscale *Lenna* image in a) are extracted using the mentioned detectors, their results being displayed in b) to g). The edge map produced by the proposed multi-scale detector for $K = 12$ looks much better than the edge detection output of Roberts, Sobel and Prewitt operators and even more natural than that produced by Canny method.

5. CONCLUSIONS

A novel and effective image boundary detection technique has been developed using the anisotropic diffusion-based multi-scale analysis. Although we have performed much research in the multi-scale and PDE-based image processing and analysis fields in the last 15 years [20, 21], the diffusion-based multi-scale edge detection domain has not been seriously approached by us until now. Thus, the automatic edge detector described here represents a new direction in our PDE-based image analysis research, combining the multi-scale analysis to nonlinear diffusion equations. It makes a much better edge detection solution than our past PDE-based single-scale approaches [18]. While its components are inspired by our previous PDE-based multiscale analysis results, they represent new anisotropic diffusion schemes and scale-space models.

So, the scale-space representation that has been created by using a non-variational well-posed nonlinear second-order diffusion model proposed here represents the main contribution of this research paper. A stable approximation algorithm that is consistent to the PDE-based model and solves it numerically by converging to its variational solution is constructed by applying the finite difference method and then used to create the scale-space. The edge detection procedure that is applied at each scale and the fine-to-coarse tracking technique that combines successfully the boundaries identified at multiple scales represent other new contributions of this research. The performed edge detection simulations and method comparisons illustrate the effectiveness of the proposed approach and the benefits of the multi-scale image analysis using nonlinear diffusion schemes in the boundary extraction field. The PDE-based multi-scale edge detector presented here outperforms clearly the single-scale edge detection methods, especially for the natural images, and also provides better results than multi-scale techniques based on Gaussian filters, given the much better preservation of the edge strength and localization provided by the anisotropic diffusion filtering.

The proposed edge detection framework can be applied successfully to image segmentation, since very good region segmentation results could be achieved by linking the edges detected by it. The segmentation results can be next applied to other computer vision areas that have been also widely investigated by us, such as the face detection [27] or the object detection and tracking [28]. Also, this automatic multi-scale technique could be transformed it into an improved multi-resolution edge detection method, by considering a different image resolution at each scale and creating an anisotropic diffusion-based pyramid as scale-space. This method improvement and its application fields will make the focus of our future research.

REFERENCES

1. D. ZIOU, S. TABBONNE, *Edge detection techniques: An overview*, International Journal of Pattern Recognition and Image Analysis, **8**, 4, pp. 537–559, 1998
2. G.N. CHAPLE, R.D. DARUWALA, M.S. GOFANE, *Comparisons of Robert, Prewitt, Sobel operator based edge detection methods for real time uses on FPGA*, 2015 International Conference on Technologies for Sustainable Development (ICTSD), Mumbai, India, pp. 1-4, 2015.
3. R. HARALICK, *Digital step edges from zero crossing of second directional derivatives*, IEEE Transactions on Pattern Analysis and Machine Intelligence, **6**, 1, pp. 58–68, 1984.
4. D. MARR, E. HILDRETH, *Theory of edge detection*, Proceedings of the Royal Society of London, Series B: Biological Sciences, **207**, 1167, pp. 187–217, 1980.
5. J. CANNY, *A computational approach to edge detection*, IEEE Transactions on Pattern Analysis and Machine Intelligence, **8**, pp. 679–714, 1986.
6. X. REN, *Multi-scale improves boundary detection in natural images*, European Conference on Computer Vision, Springer, Berlin, Heidelberg, 2008, pp. 533–545.
7. A.P. WITKIN, *Scale-space filtering*, International Joint Conference on AI, pp. 1019–1022, 1983.
8. X. ZHUANG, T. HUANG, *Multi-scale edge detection with Gaussian filters*, Proceedings of IEEE International Conference on Acoustics, Speech and Signal Processing (ICASSP), pp. 2047–2050, 1986.

9. F. BERGHOLM, *Edge focusing*, IEEE PAMI, **9**, 6, pp. 726–741, 1987.
10. J. WILLIAMS, M. SHAH, *Edge contours using multiple scales*, Computer Vision, Graphics, and Image Processing, **51**, 3, pp. 256–274, 1990.
11. C. LOPEZ-MOLINA, B. DE BAETS, H. BUSTINCE, J. SANZ, E. BARRENECHEA, *Multiscale edge detection based on Gaussian smoothing and edge tracking*, Knowledge-Based Systems, **44**, pp. 101–111, 2013.
12. Y. LI, Y. BI, W. ZHANG, C. SUN, *Multi-scale anisotropic Gaussian kernels for image edge detection*, IEEE Access, **8**, pp. 1803–1812, 2019.
13. W.F. MA, C.X. DENG, *An improved wavelet multi-scale edge detection algorithm*, 2012 International Conference on Wavelet Analysis and Pattern Recognition, IEEE, pp. 302–306, 2012.
14. W. SUN, J. SONG, L. ZHANG, *Wavelet multi-scale edge detection using adaptive threshold*, 2009 5th International Conference on Wireless Communications, Networking and Mobile Computing, IEEE, pp. 1–4, 2009.
15. P. PERONA, J. MALIK, *Scale-space and edge detection using anisotropic diffusion*, IEEE Transactions on pattern analysis and machine intelligence, **12**, 7, pp. 629–639, 1990.
16. D. MUMFORD, J. SHAH, *Boundary detection by minimizing functional*, International Conference on Computer Vision and Pattern Recognition, San Francisco, CA, USA, pp. 22–26, 1985.
17. X. BRESSON, *Image segmentation with variational active contours*, EPFL, 2005.
18. T. BARBU, *Segmentation-based non-texture image compression framework using anisotropic diffusion models*, Proceedings of the Romanian Academy, Series A, **20**, 2, pp. 122–130, 2019.
19. T. BARBU, *Robust contour tracking model using a variational level-set algorithm*, Numerical Functional Analysis and Optimization, **35**, 3, pp. 263–274, 2014.
20. T. BARBU, *Novel diffusion-based models for image restoration and interpolation*, Book Series: Signals and Communication Technology, Springer International Publishing, 2019.
21. T. BARBU, *Automatic unsupervised texture recognition framework using anisotropic diffusion-based multi-scale analysis and weight-connected graph clustering*, Symmetry, **13**, p. 925, 2021.
22. P. JOHNSON, *Finite difference for PDEs*, course, School of Mathematics, University of Manchester, Semester I, 2008.
23. P. SOILLE, *Morphological image analysis: principles and applications*, 2nd edition, Springer Verlag, Berlin, 2003.
24. T.Y. ZHANG, C.Y. SUEN, *A fast parallel algorithm for thinning digital patterns*, Commun. ACM **27**, pp. 236–239, 1984.
25. A.P. KHAIRE, N.V. THAKUR, *A fuzzy set approach for edge detection*, International Journal of Image Processing (IJIP), **6**, 6, pp. 403–412, 2012.
26. D. MARTIN, C. FOWLES, D. TAL, J. MALIK, *A database of human segmented natural images and its application to evaluating segmentation algorithms and measuring ecological statistics*, Proceedings of ICCV '01, pp. 416–425, 2001.
27. T. BARBU, *An automatic face detection system for RGB images*, International Journal of Computers, Communications & Control, **6**, 1, pp. 21–32, 2011.
28. T. BARBU, *SVM-based human cell detection technique using histograms of oriented gradients*, In: *Mathematical Methods for Information Science & Economics*, Proceedings of the 3rd International Conference for the Applied Mathematics and Informatics (AMATHI'12), Montreux, Switzerland, December 29-31, 2012, pp. 156–160.

Received March 28, 2021